Journal of Ethnopharmacology 282 (2022) 114637

Contents lists available at ScienceDirect

Journal of Ethnopharmacology

journal homepage: www.elsevier.com/locate/jethpharm

The modulatory role of prime identified compounds in *Geophila repens* in mitigating scopolamine-induced neurotoxicity in experimental rats of Alzheimer's disease via attenuation of cholinesterase, β-secretase, MAPt levels and inhibition of oxidative stress imparts inflammation

Umesh Chandra Dash [a], Sandeep Kumar Swain [a], Satish Kanhar [a], Purusottam Banjare [b], Partha Pratim Roy [b], Jagneshwar Dandapat [c], Atish Kumar Sahoo [a,*]

[a] Regional Plant Resource Centre, Medicinal & Aromatic Plant Division, Forest & Environment Department, Govt. of Odisha, Nayapalli, Bhubaneswar, 751015, India
[b] Division of Pharmaceutical & Medicinal Chemistry, Institute of Pharmacy, Guru Ghasidas University, Bilaspur, 495009, Chhattisgarh, India
[c] Department of Biotechnology, Utkal University, Vani Vihar, Bhubaneswar, 751004, India

ARTICLE INFO

Keywords:
Geophila repens
Cholinesterase
β-secretase
MAPt
Molecular docking
Alzheimer's disease

ABSTRACT

Ethnopharmacological relevance: Geophila repens (L.) I.M. Johnst (Rubiaceae) is a small perennial creeper native to India, China, and other countries in Southeast Asia. The hot decoction of leaves is used orally for memory enhancing by the local folk of Andhra Pradesh, India. The ethnomedicinal claim of *G. repens* as memory enhancer was initially studied by the authors. Results demonstrated the important antioxidant and anticholinesterase activities of isolated molecule Pentylcurcumene and bioactive hydroalcohol extract of leaves of *G. repens* (GRHA).

Aim of the study: Based on the previous findings, additional research is needed to examine the efficacy of GRHA for memory enhancing properties. We therefore investigated the modulatory role of prime identified compounds in GRHA in mitigating scopolamine-induced neurotoxicity in experimental rats of Alzheimer's disease (AD) via attenuation of cholinesterase, β-secretase, MAPt levels and inhibition of oxidative stress imparts inflammation.

Methods: Scopolamine (3 mg/kg) induced experimental rats of AD were treated with GRHA (300, 400 mg/kg) for 14 days. During the experimental period, elevated T-maze and locomotion-activity were performed to assess learning and memory efficacy of GRHA. At the end of the experiment, biochemical, neurochemical, neuro-inflammation and histopathological observation of brain cortex were examined. GC-MS/MS analysis reported 31 compounds, among them 8 bioactive compounds possess antioxidant, neuroinflammation, neuroprotective activities, and were considered for docking analysis towards cholinesterase, β-secretase activities in AD.

Results: GRHA 400 significantly improved learning and memory impairment with the improvement of oxidative stress (MDA, SOD, GSH, CAT), DNA damage (8-OHdG), neurochemical (AChE, BuChE, BACE1, BACE2, MAPt), neuroinflammation (IL-6, TNF-α) markers in neurotoxic rats. Docking studies of 8 compounds demonstrated negative binding energies for cholinesterase and β-secretase indicating high affinity for target enzymes in AD. Test results were corroborated by the improvement of cellular tissue architecture of brain cortex in AD rats.

Conclusion: Synergistic action of genistin, quercetin-3-D-galactoside, 9,12,15-octadecatrienoic-acid methyl-ester, phytol, retinal, stigmasterol, n-hexadecanoic acid, β-sitosterol in GRHA restores memory-deficits via attenuation of cholinesterase, β-secretase, MAPt level and inhibition of oxidative-stress imparts inflammation in AD.

1. Introduction

Alzheimer's disease (AD) is a type of incurable and progressive neurodegenerative disorder characterised by formation, aggregation and accumulation of amyloid (Aβ)-plaque and neurofibrillary tangles (NFTs), production of inflammatory cytokines, impaired calcium homeostasis leading to cognitive decline and senile dementia. It is an acquired cognitive and behavioural impairment disorder associated with memory impairment, thinking abilities, judgement, limited social skills

* Corresponding author.
E-mail address: atish_kumar1976@yahoo.co.in (A.K. Sahoo).

https://doi.org/10.1016/j.jep.2021.114637
Received 27 July 2021; Received in revised form 6 September 2021; Accepted 10 September 2021
Available online 14 September 2021

Abbreviations

AChE	Acetylcholinesterase
AD	Alzheimer's disease
APP	amyloid precursor protein
BACE1	β-secretase 1
BACE2	β-secretase 2
BuChE	butyrylcholinesterase
BSA	bovine serum albumin
CAT	catalase
CPCSEA	control and supervision of experiments on animals
DPZ	donepezil
DTNB	dithiobis-2-nitrobenzoic acid
EDTA	ethylenediamine tetraacetic acid
FDA	Food and drug administration
GBD	Global burden of disease
GC-MS/MS	gas chromatography and mass spectroscopy
GRHA	hydroalcohol extract of *G. repens*
GSH	reduced glutathione
H&E	haematoxylin and eosin
IEAC	institutional animal ethical committee
MAPt	Microtubule associated protein Tau
MDA	malondialdehyde
NBT	nitro blue tetrazolium
OECD	Organisation for Economic Co-operation and Development
PBS	phosphate buffer saline
PDB	Protein Data Bank
PMS	phenazonium methosulphate
SCP	scopolamine
SOD	superoxide dismutase
TBA	thiobarbituric acid
TCA	trichloroacetic acid
WHO	World health organisation

and daily functioning. AD is the 6th leading reason of fatality (GBD, 2016 Neurology Collaborators, 2019) and the total number of people living with dementia is estimated to reach 82 million by 2030. The pathogenic cause of AD remains incompletely understood, however various underlying factors e.g., cholinergic dysfunction (Acetylcholinesterase and butyrylcholinesterase), amyloid or tau toxicity (β-secretase 1, and β-secretase 2), phosphorylated Tau protein (MAPt), oxidative stress, and mitochondrial dysfunction are attributed to the pathophysiology of AD (Francis et al., 1999). Oxidative stress plays a crucial role in etiopathogenesis of AD causes an imbalance in the redox homeostasis of brain cells (abundance of highly peroxidisable substrates) which is extremely vulnerable to reactive oxygen species (ROS) due to its high consumption for O_2. There is no potential drug for the treatment of AD, however Food and Drug Administration (FDA) approved synthetic (rivastigmine, velnacrine), or natural compounds (galanthamine from *Galanthus* spp.) are the partial inhibitors of enzyme activities in brain. Because of complex pathogenic features, single modality of "One-molecule one-target" strategy for treating AD has failed, and unfortunately, synthetic drugs have been linked with numerous adverse effects such as anorexia, vomiting, insomnia and nausea due to nonspecific interaction with non-targeted organ. Recent studies have focused on multi-target therapeutic strategy of bioactive fraction of botanicals to block the progression and disease-inducing mechanisms in AD (Sahoo et al., 2018).

Geophila repens (L.) I.M. Johnst belongs to Rubiaceae is a small perennial creeper native to India, China, and other countries in Southeast Asia. The hot decoction of leaves/aerial parts are used orally for inflammation, enlargements of the spleen and memory enhancing properties (Sivarajan and Balachandran, 1994; Subramoniam et al., 1998). Previous studies have almost exclusively focused on antioxidant, and anticholinesterase activities of *G. repens* as a memory enhancer. Bioautography test was employed to determine *in situ* localization and quick assessment to cholinesterase inhibitors in *G. repens* and target-directed isolation and quantification of Pentylcurcumene was reported in a complex bioactive fraction of *G. repens* (Dash and Sahoo, 2017; Dash et al., 2019). Based on the previous findings, more work is needed to analyse the safety, efficacy and toxicity of hydroalcohol fraction of leaves of *G. repens* (GRHA) and identifying the novel bioactive compounds in mitigating scopolamine-induced neurotoxicity in rat model of AD.

Scopolamine (SCP)-induced memory impairment is one of the most extensively used models in disrupting the cholinergic system e.g., memory deficiencies, cognitive decline, and impairment in special learning (Lee et al., 2018). To assess the preclinical test of exploratory and locomotor activities, memory and learning efficiency in SCP-induced neuropathy in AD rats, the elevated T-maze and locomotion activity tests were carried out. To find out the molecular mechanism action of GRHA, neurotransmitters/proteins (AChE, BuChE, β-secretase e.g., BACE1, BACE2, and MAPt) levels were studied. Oxidative stress and brain inflammation are a common denominator to initiate and promote multiple etiologies of AD. In fact, high levels of pro-inflammatory cytokines e.g., interleukin-6 (IL-6), tumour necrosis factor-alpha (TNFα) have been detected in the brain of AD patients (Hesse et al., 2016). 8-hydroxy-2′-deoxyguanosine (8-OHdG) is an endogenous oxidative DNA damage biomarker and it is used to measure various pathological conditions associated with oxidative stress-induced neurodegeneration, inflammation. The study highlights the interrelation between oxidative stress induced pathophysiological markers e.g., AChE, BuChE, BACE1, BACE2, MAPt, inflammation (IL-6, TNF-α) and DNA damage biomarker (8-OHdG) in the brain and evaluation of possible mechanism of bioactive molecules in mitigating of SCP-induced cellular stress in experimental rats via attenuation of oxidative stress imparts inflammation. GC-MS/MS analyses the presence of key bioactive components and *in silico* molecular docking analysis were carried out towards key enzymes (AChE, BuChE, BACE1, and BACE2) and binding affinity/energy in AD were reported. Histopathological studies of cortex of brain were performed to assess the neuroprotection of GRHA.

2. Material and methods

2.1. Chemicals and reagents

Scopolamine hydrobromide (SCP), Donepezil (DPZ), dithibis-2-nitrobenzoic acid (DTNB), GSH, phenazonium methosulphate (PMS), thiobarbituric acid (TBA), thiobarbituric acid (TBA), ethylenediamine tetraacetic acid (EDTA), nitro blue tetrazolium (NBT), trichloroacetic acid (TCA), hydrogen peroxide (H_2O_2), triton-X-100, Ferric chloride, hydroxylamine hydrochloride, and bovine serum albumin (BSA) were purchased from Sigma Aldrich, USA and SRL Pvt. Ltd., India. IL-6, TNF-α, BACE1, BACE2 and MAPt ELISA kits were purchased from Wuhan Fine Biological Technology Co., Ltd., China and all analytical grade solvents were procured from SRL Pvt. Ltd., Mumbai, India.

2.2. Plant material collection and preparation of bioactive fraction

Aerial parts of *Geophila repens* (L.) I.M. Johnst (Rubiaceae), were collected from Barbara Forest, Khurda district, Odisha, India (19° 52′ 53.9″N, 85° 03′ 26.2″E) and with the taxonomic authentication by Dr. P. C. Panda, Taxonomist, Regional Plant Resource Centre, Bhubaneswar, it was matched with the earlier deposited voucher specimen at our Centre

(7557/RPRC). The shade dried leaf powered material was percolated by extracting with hydroalcohol (70% ethanol) at room temp for 72 h. Extracted hydroalcohol fractions of *G. repens* (GRHA) were vacuum distillation by rotary-vacuum evaporator (R-100, Buchi, Switzerland), and % yield of GRHA was obtained (7.5% w/w) (Dash et al., 2019).

2.3. Gas chromatography-mass spectrometry (GC-MS/MS) analysis of GRHA

GC-MS/MS analysis of GRHA was performed (Bruker, SCION 436-GC); equipped with triple quadrupole-MS detector with attached column (BR-5MS; 30 m × 0.25 mm × 0.25 μM, diphenyl; 5%, dimethyl polysiloxane; 95%) and an EIS sensor (positive ionization mode; 70 eV). To maintain the constant flow rate (1 mL/min) of injected sample (2 μL, split ratio 10:1), helium (99.999%) was used as carrier gas. The injection temp was 260 °C and 250 °C in spilt mode. The temp of oven was set to 110 °C withhold time of 3.50 min through the temp rise 10 °C/min up to 200 °C and then 5 °C/min up to 280 °C for 12 min (Total running time: 40.50 min). The mass fragmentation (m/z) was set to 50–500 amu and solvent delay time was 0–3.5 min. The inlet line temp was set at 290 °C and on the basis of the relative %, each component was reported. The compounds were identified by comparing respective mass spectra with the National Institute of Standards and Technology (NIST) version 11 database and the chromatograms were programmed accordingly (MS station 8) (Kanhar et al., 2018).

2.4. Molecular docking analysis

Molecular docking analysis was performed by using LibDock (Discovery studio) software and the bioactive compounds were docked with AChE, BuChE, BACE1, and BACE2. Charm force field was applied for the energy minimization of compounds. The structure of the bioactive compounds of GRHA were retrieved from PubChem database and the selected compounds with Pubchem CIDs were dichloroacetic acid, tridec-2-ynyl ester (531,238), 6-hydroxymethylbicyclo [2.2.1]hept-2-ene-1-carboxylic acid, methyl ester (580,050), phytol (5,280,435), n-hexadecanoic acid/palmitic acid (985), β-sitosterol (222,284), quercetin 3-D-galactoside (5,281,643), stigmasterol (5,280,794), genistin (5,281,377) and donepezil (3152). They were given ~100 of docking poses for each ligand and best pose was selected for each ligand on the basis of their docking score and binding energy. The protein structure of AChE (4RVK, 1.85 Å), BuChE (6EQQ, 2.40 Å), BACE1 (5UYU, 1.9 Å) and BACE2 (3 ZKS, 2.11 Å) were retrieved from Protein Data Bank (PDB). The protein structures were refined by addition of missing amino acid residue, removal of water molecules, and minimizing energy. Finally, the active site (bound ligand site) was selected for docking the ligands. The active site selection was done by clicking “from PDB site record”. The visualization of docking analysis was done by Discovery studio (Client version 4.5) and based on the binding energy; the interactions were calculated (Jamila et al., 2015).

2.5. Experimental animals

2.5.1. Animals

The protocol for conducting animal experiment was approved by the Institutional Animal Ethics Committee (IAEC) of Regional Plant Resource Centre, Bhubaneswar, and the experiment was carried out in accordance with the guidelines of the Committee for the Purpose of Control and Supervision of Experiments on Animals (CPCSEA), New Delhi, India (Regd. No. 1807/GO/R/S/15/CPCSEA). Wistar rats of either sex (weighing 150–200 g, 4 months old) was purchased from Imgenex India Pvt. Ltd., Bhubaneswar, India and not more than 6 animals were kept in a well ventilated specific designed polypropylene cages at 25–30 °C under 12 h light/dark cycles. Rats were fed with standard rodent diet and water *ad libitum*. Prior to the experiments, rats were acclimatized for a week to laboratory conditions to nullify the psychological sickness during transportation and handling stress.

2.6. Acute toxicity study of GRHA

The test guidelines for determination of acute toxicity (LD_{50}) of GRHA was followed by OECD guidelines. Animals were divided into 5 groups (n = 6) and were fasted overnight. Oral single administration of GRHA dose (500, 1000, 2000, 3000 and 4000 mg/kg, b.w.) to different groups to determine the effective dose. Rats in different groups were under supervision for any change in sign and symptoms includes alertness, gait, touch response, fearfulness, restlessness, irritability, urination, defecation and death within 72 h (Kanhar et al., 2018).

2.7. Experimental procedures

The rats were randomly divided into 5 groups (n = 6/group).

Group 1 (normal control): received normal saline (n.s.)
Group 2 (Scopolamine/SCP-induced): received scopolamine hydrobromide (3 mg/kg, i.p.)
Group 3 (Donepezil/DPZ treated): received SCP + DPZ (2 mg/kg, p.o.)
Group 4 (GRHA-300): received SCP + GRHA-300 (300 mg/kg, p.o.)
Group 5 (GRHA-400): received SCP + GRHA-400 (400 mg/kg, p.o.)

Rats were trained and after acquisition of trial, rats were subjected to behavioural studies. The group 1 and 2 rats were treated with normal saline daily (n.s.; p.o.), and SCP (3 mg/kg, i.p.), respectively. Group 3, 4, and 5 were treated with DPZ (2 mg/kg, p.o.), low dose of GRHA (GRHA-300; 300 mg/kg, p.o.) and high dose of GRHA (GRHA-400; 400 mg/kg, p.o.), respectively at every 24 h interval for 14 consecutive days. The behavioural analysis of all groups was carried out 30 min prior to dose administration during experimental days. After completion of the behavioural tests, on the 15th day rats were sacrificed. Blood serum and whole brain of each experimental rat were collected. Oxidative stress markers (MDA, SOD, GSH, and CAT), DNA damage biomarker (8-OHdG), and inflammatory markers (IL-6, TNF-α) of serum and brain were estimated. Neurochemical estimation (AChE, BuChE, BACE1, BACE2, and MAPt) and histopathological studies of brain tissues were performed (Upadhyay et al., 2020).

2.8. Behavioural analysis

2.8.1. T-maze test

Prior to the experiment, the animals were habituated in T-maze apparatus for a period of 10 min. One of the arms of the apparatus was selected as preferred arm and other one was discriminated arm. In acquisition period, food was kept in preferred arm and discriminated arm was closed. Animals were kept in the starting arm and allowed to move towards the open arm. In retention period, rats in group 1, group 2, and group 3 were administered with distilled water, scopolamine (3 mg/kg) and donepezil (2 mg/kg), respectively. The experimental groups (group 4, and 5) were administered with 300 and 400 mg/kg dose of GRHA. After 30 min of administration, animals were placed one after the other into the T-maze for a period of 5 min. After each entry, the apparatus was cleaned with alcohol (70%) to remove the odour traces of the previous animal. Different behavioural patterns of animals were monitored by analysing different parameters e.g., time spent in different arms (preferred and discriminated), latency time to choose the preferred arm and number of entries in different arms (preferred and discriminated) were recorded (Yadang et al., 2020).

2.8.2. Locomotion activity in open field

Locomotion activity was performed by using the open field apparatus. The apparatus was made up of wooden ply (open from top and bottom, dimension 50 × 50 × 40 cm), and placed on white table top. The

table surface was divided into 25 squares of equal size (9 central and 16 peripheral). Each animal was placed in the corner of the open field model, and its behaviour was recorded for 5 min, including rearing, ambulation (number of squares entered with both forelimbs), and preening (Bhosale et al., 2011).

2.9. Collection of blood serum and preparation of tissue homogenate

After completion of behaviour analysis, animals were anesthetized (1% pentobarbital) and sacrificed on the 15th day. Blood samples were collected (retro-orbital sinus of rats) in an EDTA coated tubes and centrifuged at 3000 rpm (5424 R, Eppendorf, Germany) for 15 min at 25 °C, and the serum obtained was stored at −20 °C for the determination of oxidative stress and inflammatory markers. The whole brain was excised quickly, cleaned with ice-cold normal saline and stored at −80 °C (U410-86, Eppendorf, Germany). A small piece of brain tissue was homogenized in 10X PBS, and centrifuged (4000 rpm, 10 min) (5424 R, Eppendorf, Germany) to eliminate the extracellular debris to get non-contaminated supernatant (Upadhyay et al., 2020). The collected supernatant was kept at −86 °C deep freezer for neurochemical estimation and determination of oxidative stress and inflammatory markers. The other portion of the brain tissue was fixed with 10% formalin for histopathological analysis.

2.10. Effects of GRHA on antioxidant marker enzymes in serum and brain

The net content of MDA in each rat was determined as nM/mg protein of serum/brain by multiplying molar coefficient of 1.56×10^5 $M^{-1}cm^{-1}$ (Wright et al., 1981). The inhibition of SOD activity was estimated, and the rise in absorbance per min was determined as U/mg of protein of serum/brain (Rajashri et al., 2020). The standard method was used to estimate the GSH content, and values were expressed in mM/mg protein (Ellman, 1959). The ingesting capacity of H_2O_2 by CAT was determined with slight modifications of procedure (Rajashri et al., 2020), and the decreases in absorbance values (1 min interval) were expressed as U/mg protein.

2.11. Effects of GRHA on 8-hydroxy-2-deoxyguanosine (8-OHdG) in serum and brain

The standard method was used to determine the concentration of 8-OHdG in serum and brain (Woo et al., 2020; Zhang et al., 2018). The oxidative DNA damage of serum and brain tissues were analyzed by using 8-OHdG rat-ELISA kit (Fine Biological Technology Co., Ltd., Wuhan, China). The absorbance of unknown samples was measured at 450 nm by ELISA reader (Synergy H1MF, BioTek, USA) and 8-OHdG content of unknown samples was determined by comparison with standard curve. It follows the principle of sandwich ELISA to detect the level of 8-OHdG in serum and brain with their respective antibodies. The 8-OHdG concentration in serum and brain were calculated and expressed in ng/mL and ng/mg tissue respectively.

2.12. Effects of GRHA on inflammatory markers in serum and brain

The inflammation markers IL-6, and TNF-α of serum and brain were estimated (Fine Biological Technology Co., Ltd., Wuhan, China). It follows the principle of sandwich ELISA to detect IL-6, and TNF-α concentration in tissue supernatant (antigen) with their respective antibodies. Absorbance of final reaction mixture was measured at 450 nm using ELISA reader (Synergy H1MF, BioTek, USA), and results were presented in ng/mL.

2.13. Neurochemical analysis

2.13.1. Effects of GRHA on AChE and BuChE level in brain

Acetylcholinesterase (AChE) and butyrylcholinesterase (BuChE) content in the brain were estimated (Ellman et al., 1961). The reaction mixture was prepared by mixing 100 μL of supernatant, 75 μL of DTNB (3 mM), and 75 μL of Tris-HCl (50 mM; pH 8.0). The reaction was initiated by adding 25 μL (15 mM) of acetylcholine iodide (ATCI)/S--butyrylthiocholine chloride (SBTC) to the reaction mixture for estimation of AChE/BuChE, respectively. The changes in absorbance were recorded at 405 nm at every 1 min interval up to 10 min in a multimode microplate reader (Synergy H1MF, BioTek, USA). AChE and BuChE activities were expressed (nM/min/g protein). The above reactions were made in triplicate, and the rate of enzyme activity was calculated.

$$R = 5.74 \times 10^{-4} \times A/CO$$

Where, R = rate of moles of substrate hydrolysed/minute/g tissue;

A = change in absorbance/min; and CO = actual concentration of the tissue in mg/mL

2.13.2. Effects of GRHA on β-secretase and MAPt level in brain

The level of β-secretase (BACE1, and BACE2), and MAPt in brain tissues were estimated by rat ELISA kit (Fine Biological Technology Co., Ltd., Wuhan, China). It follows the principle of sandwich ELISA to detect the level BACE1, BACE2, and MAPt in the tissue supernatant (antigen) with their respective antibodies. Absorbance of final reaction mixture was measured at 450 nm using ELISA reader (Synergy H1MF, BioTek, USA), and results were presented in ng/mL.

2.14. Histopathological examination

The brain tissues of all experimental rats were fixed in 10% formalin (neutral buffered) for 24 h before being rinsed with running tap water. Tissues were dehydrated with increasing grades of absolute alcohol i.e., 50%, 70%, 95% and 100%, and rinsed with distilled water. Then the dehydrated tissues were embedded with paraffin blocks and sliced thick sections (5 μ) by using microtome (MRM-ST, Medimeas, India) followed by haematoxylin, and eosin (H&E) staining (Swain et al., 2020). The processed brain slices were mounted in clean glass slides and cellular architecture (neuroinflammation, pyramidal neurons, glial cells, necrotic cells, and eosinophil cells) were visualised under inverted microscope (40X; LYNX NIB 100, Lawrence & Mayo, India).

2.15. Statistical analysis

The results were expressed as mean ± SD (n = 6). The means of two groups were compared using Student's t-test. GraphPad software (Prism 7) was used for statistical analysis by one-way ANOVA and Tukey's multiple comparison test between the groups ($p < 0.05$) and identified as significant ($p < 0.001$).

3. Results and discussion

3.1. Identification of bioactive compounds by GC-MS/MS analysis of GRHA

GC-MS analysis identified the presence of 31 no. of compounds of different class such as flavone, terpene, ester, steroid and aldehydes in GRHA (Fig. 1). The chromatograms of identified compounds were compared with NIST mass spectral library and reported with their respective molecular formula, molecular weight, peak number, retention time (RT), nature of compound, and biological activities. The major identified compounds were genistin, ascaridole epoxide, quercetin-3-D-galactoside or hyperoside, 2(3H)-naphthalenone 4,4a,5,6,7,8-

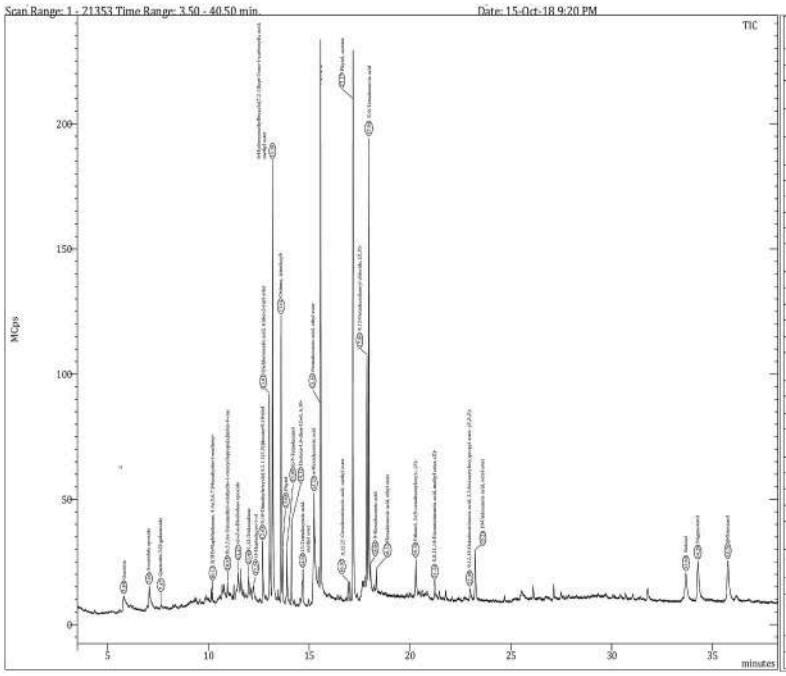

Sl. No.	Compounds Name	Molecular formula	Molecular weight	Nature of compound	Retention time	Pharmacological activities	Reference
1.	Genistin	$C_{21}H_{20}O_{10}$	432	Flavone	5.84	Alzheimer's disease	Uddin and Kabir, 2019
2.	Isoarctiide epoxide	$C_{15}H_{24}O_2$	164	Terpene	7.88	-	
3.	Quercetin 3-B-galactoside	$C_{21}H_{20}O_{12}$	464	Flavone	7.47	Neuroprotection; Antipsia and Anti-inflammation	Zeng et al., 2011
4.	2,(1H)-Naphthalenone, 4,4a,5,6,7,8-hexahydro-1-methoxy-	$C_{11}H_{18}O_2$	180	Cyclic hydrocarbon	10.33	-	
5.	1b,5,5,6a-Tetramethyl-octahydro-1-oxacyclopropa[a]inden-6-one	$C_{15}H_{24}O_2$	208	Cyclic hydrocarbon	10.95	-	
6.	cis-Z-α-Bisabolene epoxide	$C_{15}H_{24}O$	220	Cyclic hydrocarbon	11.47	-	
7.	1,12-Tridecadiene	$C_{13}H_{24}$	180	Hydrocarbon	11.99	-	
8.	13-Heptadecyn-1-ol	$C_{17}H_{32}O$	252	Alcohol	12.24	-	
9.	9,10-Dimethyltricyclo[4.2.1.1(2,5)]decane-9,10-diol	$C_{12}H_{22}O_2$	196	Alcohol	12.68	-	
10.	Dichloroacetic acid, tridec-2-ynyl ester	$C_{15}H_{24}Cl_2O_2$	306	Ester	13.01	-	
11.	6-Hydroxymethylbicyclo[2.2.1]hept-2-ene-1-carboxylic acid, methyl ester	$C_{10}H_{14}O_3$	182	Ester	13.18	-	
12.	Oxirane, tetradecyl-	$C_{16}H_{32}O$	240	Hydrocarbon	13.61	-	
13.	Phytol	$C_{20}H_{40}O$	296	Terpene	13.68	Neuropsychological disorders	Islam et al., 2018
14.	E-7-Tetradecenol	$C_{14}H_{28}O$	212	Alcohol	13.89	-	
15.	Dodeca-1,6-dien-12-ol, 6,10-dimethyl-	$C_{14}H_{26}O$	210	Alcohol	14.22	-	
16.	13-Tetradecynoic acid, methyl ester	$C_{15}H_{24}O_2$	238	Ester	14.68	-	
17.	n-Hexadecanoic acid Palmitic acid	$C_{16}H_{32}O_2$	256	Fatty acid	15.23	Neuroprotection after ischemia	Lin and Perez-Pinzon, 2013
18.	Pentadecanoic acid, ethyl ester	$C_{17}H_{34}O_2$	270	Ester	15.56	-	
19.	9,12,15-Octadecatrienoic acid, methyl ester	$C_{19}H_{32}O_2$	292	Ester	16.92	Anti-inflammatory	Al-Otaibi et al., 2020
20.	Phytol, acetate	$C_{22}H_{42}O_2$	338	Ester	17.17	-	
21.	9,12-Octadecadienoyl chloride, (Z,Z)- Linoleoyl Chloride	$C_{18}H_{31}ClO$	298	Acid chloride	17.86	-	
22.	E-9-Tetradecenoic acid/ Myristoleic Acid	$C_{14}H_{26}O_2$	226	Fatty acid	17.94	-	
23.	n-Hexadecanoic acid	$C_{16}H_{32}O_2$	254	Fatty acid	18.04	-	
24.	Hexadecanoic acid, ethyl ester	$C_{18}H_{36}O_2$	284	Ester	18.32	-	
25.	Ethanol, 2-(9-octadecenyloxy)-, (Z)-	$C_{20}H_{40}O_2$	312	Alcohol	20.28	-	
26.	5,8,11,14-Eicosatetraenoic acid, methyl ester, all-Z)-	$C_{21}H_{34}O_2$	318	Ester	21.24	-	
27.	9,12,15-Octadecatrienoic acid, 2,3-bis(acetyloxy)propyl ester, (Z,Z,Z)-	$C_{27}H_{44}O_6$	464	Ester	22.89	-	
28.	10-Undecenoic acid, octyl ester	$C_{19}H_{36}O_2$	296	Ester	23.21	-	
29.	Retinal	$C_{20}H_{28}O$	284	Aldehyde	33.69	Antioxidant and Anti-ageing	Belyaeva et al., 2019; Babamiri and Nassab, 2010
30.	Stigmasterol	$C_{29}H_{48}O$	412	Steroid	34.28	Alzheimer's disease	Bogie et al., 2019
31.	β-Sitosterol	$C_{29}H_{50}O$	414	Steroid	35.76	Alzheimer's disease	Bogie et al., 2019

Fig. 1. GC-MS/MS analysis of hydroalcohol fraction of *Geophila repens* (GRHA) and the reported compounds with biological activities.

hexahydro-1-methoxy-, 1 b, 5,5,6a-tetramethyl-octahydro-1 oxacyclopropa [a] inden-6-one, cis-Z-α-bisabolene epoxide, 1,12-tridecadiene, 13-heptadecyn-1-ol, 9,10-dimethyltricyclo [4.2.1.1 (2,5)]decane-9,10-diol, dichloroacetic acid, tridec-2-ynyl ester, 6-hydroxymethylbicyclo [2.2.1]hept-2-ene-1-carboxylic acid methyl ester, oxirane, tetradecyl, phytol, E−7-tetradecenol, dodeca-1,6-dien-12-ol, 6,10-dimethyl-, 13-tetradecynoic acid methyl ester, n-hexadecanoic acid, pentadecanoic acid ethyl ester, 9,12,15-octadecatrienoic acid methyl ester, phytol acetate, 9,12-octadecadienoyl chloride, (Z,Z) or linoleoyl chloride, E−9-tetradecenoic acid, or myristoleic acid, 9-hexadecenoic acid, hexadecanoic acid, ethyl ester, ethanol, 2-(9-octadecenyloxy)-(Z)-, 5,8,11,14-eicosatetraenoic acid methyl ester (all-Z)-, 9,12,15-octadecatrienoic acid-2,3-bis(acetyloxy)propyl ester (Z,Z,Z)-, 10-undecenoic acid octyl ester, retinal, stigmasterol, and β-sitosterol. Based on the potential therapeutic interest to cure neurological disorders, only 8 no. of bioactive compounds e.g., genistin, quercetin-3-D-galactoside or hyperoside, phytol, stigmasterol, n-hexadecanoic acid, 9,12,15-octadecatrienoic acid methyl ester, retinal, and β-sitosterol possess antioxidant, anti-inflammatory, and neuroprotective activities.

Based on the scientific evidence and current findings, a proposed mechanism of identified molecules has been described (Fig. 5). Genistin, after ingestion is hydrolysed to bioactive genistein (isoflavone) which acts as estrogen receptor β (ERβ) agonist. Genistein-ERβ binding affinity activates the signalling pathway of protein kinase C (PKC), phosphorylation of MEK, mitogen-activated protein kinase (MAPK) and IKb. It enhances the APP cleavage by improving α-secretase activity, stimulates NFkB translocation and up regulates the expression of antioxidant enzymes in oxidative stress-induced memory deficit and mitochondrial dysfunction in AD (Uddin and Kabir, 2019; Devi et al., 2017). Hyperoside (hyperin, or quercetin 3-D-galactoside) is a bioactive flavone glycoside. It exhibited anti-inflammatory activities by suppressing the production of IL-6, TNF-α and NO and also, inhibits ROS production by balancing oxidative enzymes (SOD, CAT, GSH and MDA) and prevents the release of cytochrome-c from mitochondria in caspase-dependent neuronal death. It also activates PI3K/Akt signalling pathway and prevents the translocation of Bad to mitochondria and inhibits the mitochondrial apoptosis in AD (Kim et al., 2011; Ku et al., 2014). So, this drug raises the possibility of developing into a clinically effective drug in neurodegenerative disease treatment associated with mitochondrial dysfunction (Zeng et al., 2011). Phytol is an acyclic diterpene alcohol, used to treat a variety of neuropsychological disorders e.g., anxiolytic, epilepsy and antidepression (Islam et al., 2018). Because of its strong radical scavenging activities, phytol prevents the formation of TBARS, and reduced the level of TNF-α, IL-6, and IL-8 by suppressing H_2O_2-induced inflammation in rats (Santos et al., 2013; Jeong, 2018). Previous pre-clinical studies have demonstrated that the consumption of phytol and phytol loaded poly lactic-*co*-glycolic acid nanoparticles (phytol-PLGANPs) significantly ameliorated SCP-induced cognitive deficits by improving spatial and short-term memory, enhancing the cholinergic effect by inhibiting AChE, BuChE, BACE1 activities by activating antioxidative defence system (Sethuraman et al., 2020). n-hexadecanoic acid modulates cerebral blood flow and neuroprotection with improved learning and memory recovery in rats by nicotinic acetylcholine receptors (nAChRs) mediate transmission (Carta et al., 2017; Lin and Perez-Pinzon, 2013; Aparna et al., 2012). 9,12,15-octadecatrienoic acid methyl ester is the inflammatory initiator responsible for liver injuries which normalises the expression of mRNA of cytokines (TNFα, IL-6, and IL-10) with stress gene (iNOS, HO-1) that play important roles in liver protection and liver regeneration (Al-Otaibi et al., 2020). Retinal (vitamin A aldehyde/retinaldehyde/retinene) is a potent natural anti-aging agent with great antioxidant activities activates target nuclear genes to produce retinoic acid-response related protein towards the suppression of neuroinflammation (IL-6, TNF-α), and inhibit the neural death in AD (Babamiri and Nassab, 2010; Maden, 2002). It is a direct precursor of retinoic acid, formed by oxidation of retinol in presence of retinol dehydrogenase (Belyaeva et al., 2019). Stigmasterol reduces neurological deficits and restores endogenous antioxidant defence system of ischemic injury in rat brain by preventing the autophagy activation via AMPK-mTOR, and JNK pathways in brain (Sun et al., 2019; Bogie et al., 2019). β-sitosterol has antioxidant activities of SOD, CAT, GSH and decreased the level of MDA in oxidative stress-induced ROS production. Because of its antioxidant properties, it helps in improving cognitive deficits, short term memory and locomotor disabilities in AD rat by improving mitochondrial function and decreasing ROS generation, and also prevents the damage of myelin sheaths in neurons (Adebiyi et al., 2019; Bogie et al., 2019).

3.2. Molecular docking analysis of potential bioactive compounds of anti-Alzheimer's activity

In silico molecular docking study of selected bioactive compounds e.g. dichloroacetic acid-tridec-2-ynyl ester, 6-hydroxymethylbicyclo [2.2.1]hept-2-ene-1-carboxylic acid-methyl ester, phytol acetate, n-hexadecanoic acid, β-sitosterol, quercetin-3-D-galactoside, stigmasterol, and genistin were performed to identify potential inhibitory compounds against AD associated proteins (AChE, BuChE, BACE1, and BACE2). The docking analysis was performed on four proteins retrieved from protein data bank (PDB). They are AChE (4RVK, 1.85 Å), BuChE (6EQQ, 2.40 Å), BACE1 (5UYU, 1.9 Å) and BACE2 (3 ZKS, 2.11 Å). As previously stated, protein refinement was performed for each protein, and ligands were docked in the respective active sites. Discovery Studio analysis tool was used to calculate docking score/binding energy of the molecules (Table 1) and the visualisations of protein-ligand interaction were shown (2D plot) within 3 Å (Fig. 2) which represented the hydrophobic interactions of ligands with amino acids present in active site. The closer view of Fig. 2 depicted that the ligands interacted with different amino acids (Ala, Arg, Asn, Cys, Glu, Gln, Gly, His, Ile, Leu, Lys, Met, Phe, Pro, Ser, Thr, Trp, Tyr, and Val) within the hydrophobic cavity of AChE, BuChE, BACE1 and BACE2 along with various bond interactions viz. hydrogen, alkyl, π-alkyl and Vander wall bonds etc. The molecular docking results depicted that the binding energy of quercetin-3-D-galactoside/hyperoside (−232.671) and genistin (−201.653) exhibited better activity towards AChE as similar to reference drug donepezil (−215.353). The binding energy of dichloroacetic acid-tridec-2-ynyl ester, phytol-acetate, quercetin-3-D-galactoside, genistin, β-Sitosterol and stigmasterol towards BuChE showed the higher binding energy scores as −92.913, −100.002, −218.426, −145.664, −61.881 and −80.092, respectively as found comparable to donepezil (−54.464). The bioactive compounds, dichloroacetic acid-tridec-2-ynyl ester (BACE1: 126.584; BACE2: 110.069), phytol-acetate (BACE1: 92.556; BACE2: 95.865), quercetin-3-D-galactoside (BACE1: 250.149; BACE2: 144.478), genistin (BACE1: 178.161; BACE2: 199.992), stigmasterol (BACE1: 100.711) against β-secretase exhibited better binding affinity as compared to donepezil (BACE1, -84.771: BACE2, -107.477). The above molecular docking analysis of all selected ligands with respective proteins resulted in a large change in binding free energy with various possible hydrogen and pi-alkali bond indicates *G. repens* may possibly a promising agent to block or reverse the progression of AD pathogenesis, which also supported by our *in vivo* findings (Jamila et al., 2015; Dash et al., 2019).

3.3. Acute toxicity study of GRHA

Acute toxicity study was carried out to determine the adverse effect, lethal and effective doses of GRHA. GRHA administered to experimental rats in group I to V at a dose of 500–4000 mg/kg, respectively. The rats in groups I, II and III did not show any treatment related mortality, whereas rats in group III were excessively defecated as a sign of toxicity. Within 24 h of dose administration, rats in groups IV and V showed mortality rate of 2/6 and 3/6, respectively. The survived rats in groups IV and V showed marked changes in their physiological behaviour such as excess urination, irritation and restlessness. As, half of the animals were died in group-V, LD_{50} of GRHA was recorded at 4000 mg/kg. So, two effective doses 400 and 300 mg/kg were considered to be safe for animal experimentation (Table 2A) (Kanhar et al., 2018).

3.4. Effects of GRHA on behavioural analysis

T-maze test was performed to assess protective efficacy of GRHA towards normal behavioural changes in SCP-induced AD rats. In T-maze test, the latency time, time spent and numbers of entries in different arms were measured (Table 2B). The results showed that the latency time to enter in preferred arm was significantly ($p < 0.001$) increased (29.65 ± 0.11 s) in SCP-induced group as compared to normal (9.41 ± 0.09 s). But, GRHA-400 treated group exhibited significant ($p < 0.001$) decrease in latency time (17.45 ± 0.11 s) and found comparable to DPZ treated group (12.55 ± 0.07 s). The administration of scopolamine showed significant ($p < 0.001$) decrease in time spent in the preferred arm (31.08 ± 0.24 s), and increase the latency time period in the discriminated arm (94.1 ± 0.2 s) as compared to normal (preferred arm: 62.56 ± 0.12 s; 60.16 ± 0.14 s). GRHA-400 significantly ($p < 0.001$) reversed the latency time in preferred arm (52.88 ± 0.23 s) and discriminated arm (72.61 ± 0.1 s) which were found comparable to DPZ treated group. The SCP-induced rats showed significant ($p < 0.001$) decrease in the no. of entries of rats into preferred arm (3.33 ± 0.34) and increase the no. of entries into discriminated arm (6.0 ± 0.36) as compared to normal (preferred arm: 6.5 ± 0.22; discriminated arm: 2.83 ± 0.3). But, the administration of GRHA-400 showed significant ($p < 0.001$) increase in the no. of entries of rats into preferred arm (4.83 ± 0.3) and decreased the no. of entries into discriminated arm (4.33 ± 0.42). The results were found comparable to DPZ treated group (Yadang et al., 2020).

Neuroprotective effect of GRHA was studied by measuring behavioural changes such as ambulation, rearing, and preening in the open field test (OFT). In OFT, animals were exposed to new environment, and observed for changes in normal behaviour. In SCP-induced groups, rats showed significant ($p < 0.001$) lower ambulation (peripheral: 23.5 ±

Table 1
Docking scores of GC-MS/MS analyzed compounds by using LibDock (discovery studio) software.

		AChE		BuChE		BACE1		BACE2	
		4RVK		6EQQ		5UYU		3 ZKS	
Sl. No.	Compounds	Libdock Score	Binding Energy	Libdock Score	Binding Energy	Libdock Score	Binding Energy	Libdock Score	Binding Energy
1	Dichloroacetic acid, tridec-2-ynyl ester	96.920	−87.914	125.486	−92.913	105.220	−126.584	91.937	−110.069
2	6-Hydroxy methylbicyclo [2.2.1]hept-2-ene-1-carboxylic acid, methyl ester	69.223	−52.664	87.447	−42.876	74.128	−39.895	70.649	−77.849
3	Phytol, acetate	116.664	−106.434	145.833	−100.002	125.004	−92.556	113.991	−95.865
4	n-Hexadecanoic acid/palmitic acid	98.569	−63.579	123.747	−6.065	102.918	−113.537	101.292	−22.668
5	β-Sitosterol	113.453	−87.126	91.823	−61.881	116.014	−69.633	99.803	−66.535
6	Quercetin 3-D-galactoside/hyperoside	123.881	−232.671	115.156	−218.426	113.200	−250.149	103.895	−144.478
7	Stigmasterol	112.527	−40.518	85.895	−80.092	113.339	−100.711	99.687	−80.724
8	Genistin	126.790	−201.653	136.518	−145.664	133.588	−178.161	114.824	−199.992
9	Donepezil	121.037	−215.353	127.731	−54.464	128.504	−84.771	107.771	−107.477
10	Co-Crystal	112.402	−117.476	115.051	−180.118	133.026	−89.8765	118.516	−126.127

Molecular docking analysis of 8 no. of bioactive compounds as ligand towards AD markers and their respective Libdock/binding scores compared with DPZ and co-crystal. PDB, protein data bank; AChE, acetylcholinesterase; BuChE, butyrylcholinesterase; BACE1, β-secretase 1; BACE2, β-secretase 2; DPZ, donepezil.

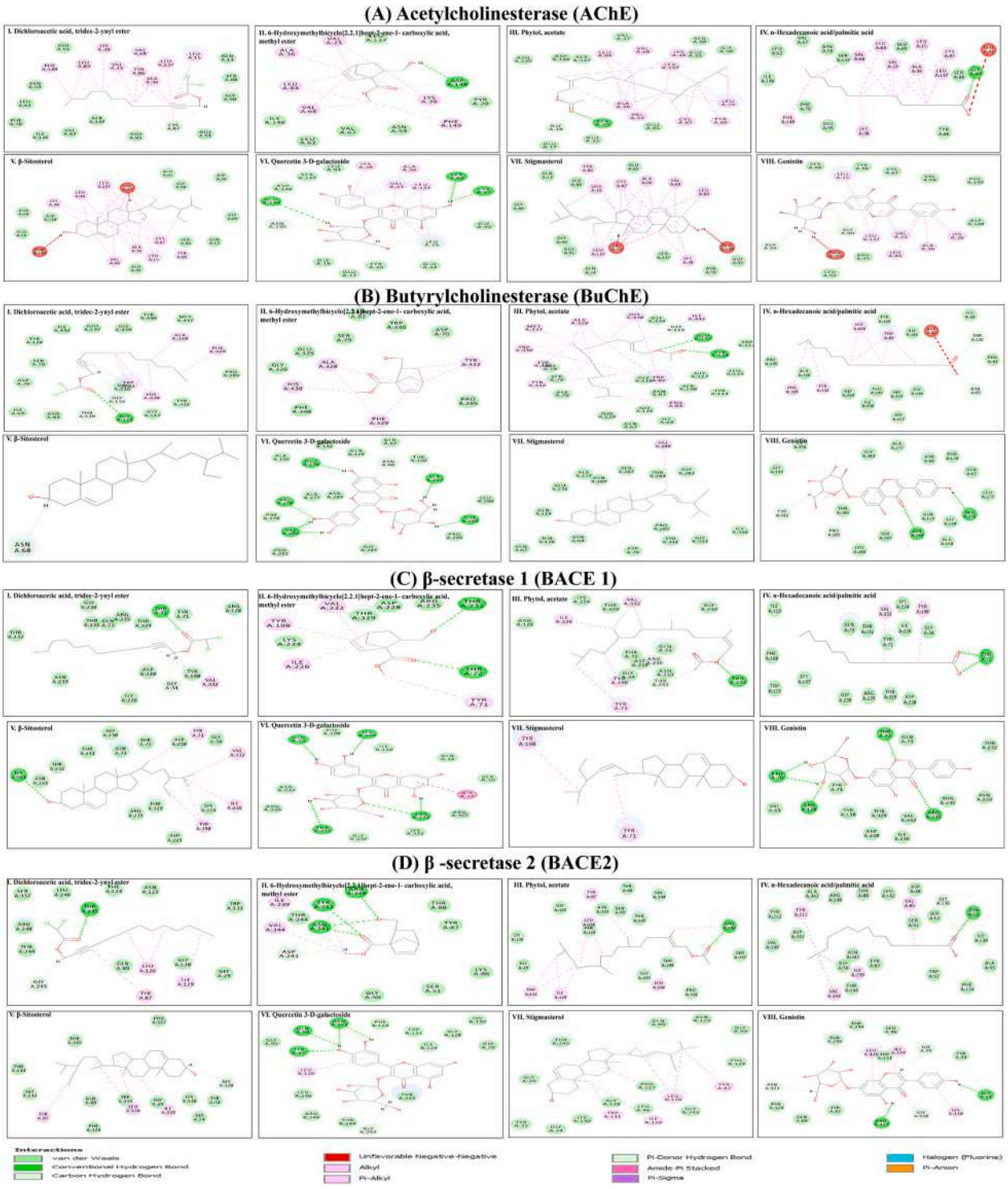

Fig. 2. Molecular docking analysis of reported bioactive compounds in GRHA towards cholinesterase and β-secretase (within 3 Å). **A and B**. Docking visualization of AChE, BuChE and their interactions with respective ligands. **C and D**. Docking visualization of BACE1, BACE2, and their interactions with respective ligands.

0.76; central: 12.5 ± 0.76), rearing (3.16 ± 0.3) and preening (2.83 ± 0.4) as compared to normal. GRHA pre-treated groups showed significant improvement ($p < 0.001$, $p < 0.01$) in ambulation (peripheral: 46.5 ± 0.76; central: 25.34 ± 0.34), rearing (7.84 ± 0.3) and preening (6.16 ± 0.3). The results were found comparable to DPZ treated group (Table 2B). GRHA-400 significantly ameliorated learning and memory deficits in SCP-induced rats due to the collective action of genistin, quercetin-3-D-galactoside, stigmasterol, phytol, 9,12,15-octadecatrienoic acid, methyl ester, retinal, and β-sitosterol (Fig. 5) which imply the cholinergic neurotransmission in the cerebral cortex and hippocampus and restore the loss of memory in AD rats (Sun et al., 2019; Bogie et al., 2019; Maden, 2002; Bhosale et al., 2011).

3.5. Effects of GRHA on oxidative markers of serum and brain

SCP-induced oxidative stress generated ROS play key roles in memory deficits and brain ageing by affecting biomolecules (lipids, nucleic acids, proteins, and carbohydrates) in cells (Birben et al., 2012).

Table 2
Acute toxicity and behaviour study of GRHA in experimental rats.

A. Acute toxicity study of GRHA in Swiss albino rats

Groups	Fraction	Dose (mg/kg)	D/T	Symptoms
I	GRHA	500	0/6	–
II		1000	0/6	–
III		2000	0/6	Defecation
IV		3000	2/6	Excess urination and irritation
V		4000	3/6	Excess urination, irritation, restlessness and death

B. Behaviour study of different rat groups by performing T-test and open field test

Groups	**T-maze test**					**Open field test**			
	Latency time (sec)	**Latency time (sec)**		**No. of entries**		**Ambulation number**		**Rearing**	**Preening**
		Preferred arm	Discriminated arm	Preferred arm	Discriminated arm	Peripheral square	Central square		
Normal control	9.41 ± 0.09	62.56 ± 0.12	60.16 ± 0.14	6.5 ± 0.22	2.83 ± 0.3	56.34 ± 0.76	31.5 ± 0.42	10.5 ± 0.67	10.33 ± 0.49
Negative control (SCP-induced)	29.65 ± 0.11$^{###}$	31.08 ± 0.24$^{###}$	94.1 ± 0.2$^{###}$	3.33 ± 0.34$^{###}$	6.0 ± 0.36$^{###}$	23.5 ± 0.76$^{###}$	12.5 ± 0.76$^{###}$	3.16 ± 0.3$^{###}$	2.83 ± 0.4$^{###}$
Positive control (DPZ-treated)	12.55 ± 0.07***	55.93 ± 0.29***	68.43 ± 0.19***	5.5 ± 0.22***	3.5 ± 0.22***	51.66 ± 0.66***	27.66 ± 0.61***	8.34 ± 0.42***	8.66 ± 0.49***
GRHA-300	21.6 ± 0.09***	45.31 ± 0.12***	84.18 ± 0.13***	3.5 ± 0.34^{ns}	4.5 ± 0.22***	37.66 ± 0.66***	18.67 ± 0.55***	5.67 ± 0.55**	4.5 ± 0.42^{ns}
GRHA-400	17.45 ± 0.11***	52.88 ± 0.23***	72.61 ± 0.1***	4.83 ± 0.3***	4.33 ± 0.42**	46.5 ± 0.76***	25.34 ± 0.34***	7.84 ± 0.3***	6.16 ± 0.3***

A. GRHA was administered (500–4000 mg/kg) to rats in group-I to V. Group I, II and III did not show any mortality, whereas rats in group III defecated showed marked sign of toxicity. Rats in groups IV and V showed mortality rate of 3/6 and 2/6, respectively within 24 h of GRHA administration. **B.** The values were represented as mean ± SD (n = 6) and one-way ANOVA (Tukey-Kramer multiple comparisons test) analysis. T-maze and Open field test were significantly ($^{###}p < 0.001$) contrived in negative control (SCP induced; 3 mg/kg b.w., i.p.) as compare to normal group. The rest of treated groups (DPZ as positive control, GRHA-300 and GRHA-400) significantly (***$p < 0.001$) improved the memory in contrast to the negative control. GRHA, hydroalcohol fraction of *Geophila repens*. D, number of animals died; T, number of treated animals.

ROS-induced lipid peroxidation causes over production of MDA and alteration in antioxidant defence enzyme (SOD, CAT, and GSH). Hence, MDA is a prime marker indicates lipid peroxidation in oxidative damage in brain cells (Haider et al., 2016). Result in Table 3 showed that the level of MDA in SCP-induced group significant ($p < 0.001$) increased (serum: 18.01 ± 0.93, and brain: 22.48 ± 2.13 nM/mg protein) as compared to normal (serum: 8.96 ± 0.66, and brain: 7.52 ± 0.33 nM/mg protein). But, pre-treatment of GRHA-400 showed significant decrease in MDA level (serum: 12.61 ± 0.78, and brain: 9.97 ± 0.52 nM/mg protein) and were found comparable to DPZ-treated rats (serum: 10.96 ± 1.12, and brain: 10.67 ± 0.54 nM/mg protein). Administration of GRHA significantly inhibited oxidative stress by balancing antioxidant enzymes and reduced the production of MDA in SCP-induced groups. SOD is the first line antioxidant defence which catalyses superoxide anion to O_2 and H_2O_2. In the present study, SOD level in SCP-induced group significantly ($p < 0.001$) decreased (serum: 5.38 ± 0.73, and brain: 4.83 ± 0.82 U/mg protein) as compared to normal (serum: 10.02 ± 0.81, and brain: 9.17 ± 0.59 U/mg protein). But, pre-treatment of GRHA-400 significantly ($p < 0.001$) increased the level of SOD (serum: 8.01 ± 0.85, and brain: 6.69 ± 0.56 U/mg protein) and found comparable to DPZ treated group (serum: 8.95 ± 0.66, and brain: 7.83 ± 0.49 U/mg protein). In SCP-induced group, oxidative stress depleted the level

Table 3
Biochemical estimation of antioxidant enzymes and neuroinflammatory markers.

Serum/ Tissue	Biochemical parameters	Normal control	Negative control (Scopolamine/SCP induced)	Positive control (Donezepil/ DPZ)	GRHA-300	GRHA-400
Serum	MDA (nM/mg protein)	8.96 ± 0.66	18.01 ± 0.93$^{###}$	10.96 ± 1.12***	14.63 ± 0.73***	12.61 ± 0.78***
	SOD (U/mg protein)	10.02 ± 0.81	5.38 ± 0.73$^{###}$	8.95 ± 0.66***	6.73 ± 0.76*	8.01 ± 0.85***
	GSH (mM/mg protein)	0.85 ± 0.05	0.19 ± 0.01$^{###}$	0.74 ± 0.01***	0.35 ± 0.02***	0.59 ± 0.03***
	CAT (U/mg protein)	50.01 ± 1.68	16.04 ± 0.92$^{###}$	45.58 ± 2.64***	35.61 ± 2.57***	40.07 ± 1.83***
	8-OHdG (ng/mL)	1.71 ± 0.07	2.92 ± 0.1$^{###}$	1.93 ± 0.05***	2.31 ± 0.15***	2.17 ± 0.11***
	IL-6 (pg/mL)	29.38 ± 2.60	61.67 ± 4.18$^{###}$	35.06 ± 2.22***	52.63 ± 2.39***	42.63 ± 2.36***
	TNF-α (pg/mL)	43.74 ± 3.64	82.97 ± 4.05$^{###}$	50.96 ± 3.31***	72.72 ± 2.55***	60.63 ± 2.95***
Brain	MDA (nM/mg protein)	7.52 ± 0.33	22.48 ± 2.13$^{###}$	10.67 ± 0.54***	12.16 ± 0.61***	9.97 ± 0.52***
	SOD (U/mg protein)	9.17 ± 0.59	4.83 ± 0.82$^{###}$	7.83 ± 0.49***	8.76 ± 0.86***	6.69 ± 0.56***
	GSH (mM/mg protein)	40.18 ± 1.48	24.11 ± 0.71$^{###}$	33.57 ± 0.89***	26.23 ± 0.93***	30.34 ± 1.04***
	CAT (U/mg protein)	58.84 ± 2.21	23.20 ± 1.77$^{###}$	50.63 ± 2.03***	38.32 ± 2.26***	47.49 ± 2.14***
	8-OHdG (ng/mg)	133.37 ± 6.21	225.67 ± 6.57$^{###}$	143.68 ± 3.24**	177.62 ± 2.89***	161.14 ± 4.4***
	IL-6 (pg/mL)	241.54 ± 18.14	711.03 ± 16.04$^{###}$	375.12 ± 6.75***	405.08 ± 7.15***	483.81 ± 9.98***
	TNF-α (pg/mL)	60.94 ± 2.89	97.41 ± 5.20$^{###}$	70.33 ± 4.71***	87.19 ± 2.72***	76.81 ± 2.61***

The values were represented as mean ± SD (n = 6) and one-way ANOVA (Tukey-Kramer multiple comparisons test) analysis were followed for all the analysis. The oxidative (MDA, SOD, GSH, CAT and 8-OHdG) and neuroinflammatory (IL-6 and TNF-α) markers status were significantly ($^{###}p < 0.001$) contrived in negative control (SCP induced; 3 mg/kg b.w., i.p.) as compare to normal control group. However, the other treated groups (DPZ as positive control, GRHA-300 and GRHA-400) significantly (***$p < 0.001$) improved the oxidative markers and restore the neuroinflammation in serum and brain tissues in contrast to the negative control. Standard drug-Donezepil/DPZ (3 mg/kg b.w., i.p.), GRHA-300, GRHA-400: hydroalcohol fraction of *G. repens* at 300 and 400 mg/kg b.w. respectively.

of GSH (serum: 0.19 ± 0.01, and brain: 24.11 ± 0.71 mM/mg protein) as compared to normal (serum: 0.85 ± 0.05, and brain: 40.18 ± 1.48 mM/mg protein), whereas GRHA-400 neutralised the over production of H_2O_2 by increasing GSH level (serum: 0.59 ± 0.03, and brain: 30.34 ± 1.04 mM/mg protein). CAT level significantly ($p < 0.001$) decreased in SCP-induced group (serum: 16.04 ± 0.92, and brain: 23.20 ± 1.77 U/mg protein) as compared to normal (serum: 50.01 ± 1.68, and brain: 58.84 ± 2.21 U/mg protein). But, GRHA-400 demonstrated significant increase ($p < 0.001$) in CAT activities (serum: 40.07 ± 1.83, and brain: 47.49 ± 2.14 U/mg protein) and found comparable to DPZ treated group (serum: 45.58 ± 2.64, and brain: 50.63 ± 2.03 U/mg protein). The current finding signified that GRHA is a potent intracellular radical scavenger to ROS and ameliorate neurological disorders in AD. This may due to the synergistic effect of radical scavengers like genistin, quercetin 3-D-galactoside, stigmasterol, phytol, 9,12,15-octadecatrienoic acid, methyl ester, retinal, and β-sitosterol in GRHA (Sethuraman et al., 2020; Bogie et al., 2019; Islam et al., 2018; Ku et al., 2014; Kim et al., 2011; Maden, 2002).

3.6. Effects of GRHA on 8-OHdG marker in serum and brain

8-hydroxy-2′-deoxyguanosine (8-OHdG) is an endogenous oxidative DNA damage biomarker. Study of 8-OHdG marker is used to measure various pathological conditions associated with oxidative stress-induced neurodegeneration, inflammation etc. Results in Table 3 showed that the level of 8-OHdG significantly ($p < 0.001$) increased (serum: 2.92 ± 0.1 ng/mL and brain: 225.67 ± 6.57 ng/mg tissue) in SCP-induced group as compared to normal (serum: 1.71 ± 0.07 ng/mL and brain: 133.37 ± 6.21 ng/mg tissue). But, pre-treatment with GRHA-400 significantly ($p < 0.001$) decreased and normalised the 8-OHdG concentrations in serum (2.17 ± 0.11 ng/mL) and brain (161.14 ± 4.4 ng/mg tissue) and found comparable to DPZ-treated group (serum: 1.93 ± 0.05 ng/mL and brain: 143.68 ± 3.24 ng/mg tissue). Similar to previous studies, a possible role of antioxidants e.g., genistin, quercetin 3-D-galactoside, 9,12,15-octadecatrienoic acid, methyl ester, stigmasterol, retinal, phytol, and β-sitosterol in GRHA inhibits lipid peroxidation, enhances enzyme antioxidant activities SOD, CAT, GSH in counteracting the oxidative stress-induced DNA damage in SCP-induced AD rat (Woo et al., 2020; Zhang et al., 2018).

3.7. Effects of GRHA on neuroinflammatory markers of serum and brain

Pro-inflammatory cytokines (IL-6 and TNF-α) play a key role in the pathological condition in CNS inflammatory diseases (neurogenesis). TNF-α is a non-glycosylated monomeric type 2 trans-membrane protein synthesized in brain by astrocytes, neurons, and microglia cells. The activated microglia cells promote the expression of pro-inflammatory cytokines and lead to cerebral neuroinflammation in AD. Moreover, activated microglia and astrocytes also generates ROS which further contributes to neurodegeneration. In the chronic neurodegenerative diseases like AD, persistent detrimental effect may result in irreversible activation of microglia which leads to persistent release of proinflammatory cytokines and ROS (Zipp and Aktas, 2006; Wang et al., 2015). Results in Table 3 showed that the level of IL-6 significantly ($p < 0.001$) increased (serum: 61.67 ± 4.18, and brain: 711.03 ± 16.04 pg/mL protein) along with the level of TNF-α (serum: 82.97 ± 4.05, and brain: 97.41 ± 5.20 pg/mL protein) in SCP-induced rats. GRHA-400 treated rats showed significant improvement in the level of IL-6 (serum: 42.63 ± 2.36, and brain: 483.81 ± 9.98 pg/mL protein) and TNF-α (serum: 60.63 ± 2.95, and brain: 76.81 ± 2.61 pg/mL protein) as similar to the standard DPZ treated rats. As illustrated in Fig. 5, the pro-inflammatory cytokine levels were decreased due to the presence of antioxidants e.g., genistin, quercetin-3-D-galactoside, stigmasterol, phytol, retinal, and β-sitosterol in GRHA may activate the Akt/ERK/-CREB synaptic proteins and supress the neuroinflammation in SCP-induced AD rats (Bogie et al., 2019; Islam et al., 2018; Zeng et al., 2011; Maden, 2002).

3.8. Effects of GRHA on cholinesterase level of brain

AChE and BuChE are found in glial cells and neurons. The key role of AChE and BuChE are to hydrolyse ACh to acetate and choline. Any disruption in these pathways leads to neurodegenerative diseases like AD. So, the major strategies to achieve the therapeutic target in the AD treatment is the inhibition of brain cholinesterase (Giacobini, 2001; Colovic et al., 2013). The rate of cholinesterase activities was estimated (Fig. 3A and B) and found that the level of cholinesterase significantly ($p < 0.001$) increased (AChE: 39.19 ± 1.86, and BuChE: 25.53 ± 1.16 nM/min/gm protein) in SCP-induced group as compared to normal (AChE: 24.01 ± 1.75, and BuChE: 15.65 ± 0.62 nM/min/gm protein). But, GRHA-400 significantly ($p < 0.001$) improved and normalised the level of cortical AChE (31.71 ± 1.46 nM/min/gm protein) and BuChE (20.61 ± 1.46 nM/min/gm protein). The results were found comparable to DPZ-treated group (AChE: 29.74 ± 1.32, and BuChE: 18.92 ± 0.89 nM/min/gm protein). The cholinesterase inhibitory effect of GRHA was due to the positive synergism in antioxidant action of genistin, quercetin-3-D-galactoside, phytol, stigmasterol and β-sitosterol towards the SCP-induced neuropathological alterations (Fig. 5) (Sun et al., 2019; Bogie et al., 2019; Islam et al., 2018; Maden, 2002). The calculated docking and binding energies also supported the cholinesterase inhibitors in GRHA by numerous molecular interactions of compounds through H-bonds to amino acid residues of AChE and BuChE.

3.9. Effects of GRHA on β-secretase (BACE1, BACE2) and MAPt level of brain

BACE1 is a typeI integral membrane protein and primarily localize in the golgi apparatus and late endosomes, which is highly expressed in brain. The second integral membrane protein BACE2 is found in very low level at peripheral tissues and mostly in astrocytes. In case of AD, the β-site amyloid precursor protein cleaving enzymes (BACE1 and BACE2) level are high and the amyloid precursor protein (APP) undergoes several cleavages in the secretory pathway to release β-amyloid peptide (Aβ) to extracellular space in brain (Irizarry et al., 2001; Basi et al., 2003). Microtubule associated protein Tau (MAPt) plays a crucial role in stabilization and formation of microtubules in neural cells to maintain its integrity and function (Barbier et al., 2019). Though the complete pathogenesis of β-secretase and MAPt in AD is not yet established but, the level of β-secretase and phosphorylated MAPt is higher in case of AD patients with unknown reason (Cole and Vassar, 2007; DeTure et al., 2019). In the present study, the level of β-secretase and MAPt were estimated (Fig. 3C and D), and found that the level of BACE1 and BACE2 significantly ($p < 0.001$) increased (BACE1: 119.31 ± 1.88, and BACE2: 14.45 ± 0.82 ng/mL protein) in SCP-induced group as compared to normal (BACE1: 106.45 ± 1.70, and BACE2: 12.34 ± 1.04 ng/mL protein). But, oral administration of GRHA-400 significantly ($p < 0.001$) decreased the BACE1 (80.89 ± 1.82 ng/mL) and BACE2 (7.68 ± 0.45 ng/mL) level and found comparable to DPZ-treated group (BACE1: 98.92 ± 1.57 and BACE2: 11.80 ± 1.00 ng/mL protein). Due to the hyperphosphorylation of MAPt, the level was decreased in SCP-induced group (7.94 ± 0.28 ng/mL) as compared to normal (14.74 ± 0.17 ng/mL). GRHA-400 significantly ($p < 0.001$) neutralised the level of MAPt (8.79 ± 0.20 ng/mL) as compared to DPZ treated group. The level of BACE1 and BACE2 were counterbalanced by the activation of PKC/MAPK/ERK 1,2 signalling pathway which can be correlated with the cumulative mode of action of genistin, quercetin-3-D-galactoside, phytol, stigmasterol and β-sitosterol in GRHA (Fig. 5) (Uddin and Kabir, 2019; Islam et al., 2018; Bogie et al., 2019). In the molecular docking study, the docking score of compounds in GRHA and the co-crystal ligands were found to be similar to standard drug Donepezil. The outcomes of *in silico* and *in vivo* shared approach of these bioactive compounds in GRHA has the potential role in balancing the increased

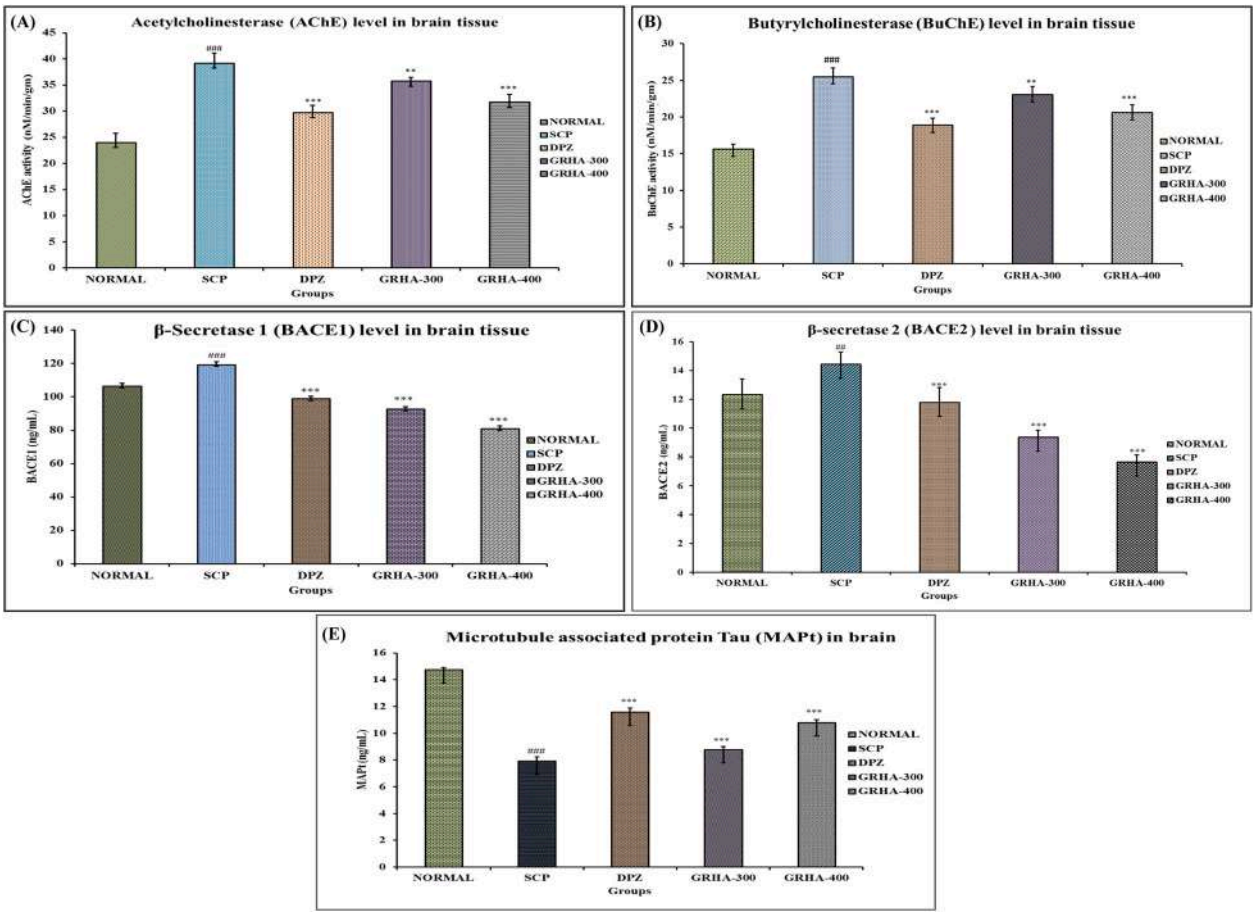

Fig. 3. The graphical representation of neuroprotective effect of GRHA-300, GRHA-400 and Donepezil/DPZ (positive control) treated groups in scopolamine (SCP)-induced AD rats. **A and B**. depicts the AChE and BuChE inhibitory activities in different groups. After SCP induction, the AChE (39.19 ± 1.86 nM/min/gm protein) and BuChE (25.53 ± 1.16 nM/min/gm protein) level were increased significantly ($^{###}p < 0.001$) as compared to normal control (AChE; 24.01 ± 1.75 and BuChE; 15.65 ± 0.62 nm/min/gm protein). However the pre-treated GRHA-400 significantly (***$p < 0.001$) decrease the level of AChE (31.71 ± 1.46 nM/min/gm protein) and BuChE (20.61 ± 1.46 nM/min/gm protein) were found comparable to DPZ treated group (AChE: 29.74 ± 1.32, and BuChE: 18.92 ± 0.89 nM/min/gm protein). **C and D**, represents the level of BACE1 and BACE2 were increased significantly (***$p < 0.001$) in SCP induced group (BACE1; 119.31 ± 1.88, BACE2; 14.45 ± 0.82 ng/mL) in comparison to normal control group (BACE1; 98.92 ± 1.57, BACE2; 11.80 ± 1.00 ng/mL). The pre-treated GRHA-400 significantly (***$p < 0.001$) balanced the BACE1 and BACE2 levels (BACE1; 80.89 ± 1.82, BACE2; 7.68 ± 0.45 ng/mL) in comparison to DPZ treated group (BACE1: 98.92 ± 1.57 and BACE2: 11.80 ± 1.00 ng/mL protein). **E.** represents the decrease level of MAPt (7.94 ± 0.28 ng/mL) in SCP-induced group in comparison to normal control (14.74 ± 0.17 ng/mL). The pre-treated GRHA-400 significantly (***$p < 0.001$) neutralise the level of MAPt (8.79 ± 0.20 ng/mL) in comparison to DPZ treated group (11.58 ± 0.29 ng/mL). The decreased level of MAPt SCP-induced group is due to the hyperphosphorylation of MAPt. All values were represented as mean ± SD (n = 6) and one-way ANOVA analysis (Tukey-Kramer multiple comparisons test) were followed for all experiments. GRHA, hydroalcohol fraction of *Geophila repens*.

level of BACE1 and BACE2 in SCP-induced rats.

3.10. Histopathological examination

In the present study, we examined the histological alterations in brain cortex of different groups in the experimental rats. The histological sections were stained with haematoxylin and eosin (H&E) to study the pathological hallmarks of AD at the cellular level. The normal control groups were showing intact glial cells (GC), neural cells (NC) and eosinophil cells (E) (Fig. 4A). In the SCP-induced group, distorted necrotic cells, shrunken glial, neural and eosinophil cells were found in scattered form which led to apoptotic changes (Fig. 4B) (Zhou et al., 2016). Although GRHA-300 showed moderate cellular improvement of glial, neural and eosinophil cells (Fig. 4D) but, a closer look to GRHA-400 treated group displayed regenerative efficiency with normal appearance of glial, neural and eosinophil cells (Fig. 4E), and found similar cellular architecture like DPZ-treated groups (Fig. 4C). The histopathological outcome revealed that GRHA-400 exhibited a significant improvement in histomorphological integrity of tissue against SCP-induced group (Rajashri et al., 2020; Sethuraman et al., 2020).

4. Conclusion

A disease modifying, multi-target neuroprotective drugs in a bioactive hydroalcohol extract of *G. repens* (GRHA) blocked the progression and disease-inducing mechanisms in AD. The therapeutic validation of GRHA at 400 mg/kg significantly improved learning and memory impairment in SCP-induced neurotoxicity in rats. It also improved the oxidative (MDA, SOD, GSH, CAT), DNA damage (8-OHdG), neurochemical (AChE, BuChE, BACE1, BACE2, MAPt), neuroinflammation (IL-6, TNF-α) markers, as evidenced by the improvement of cellular tissue architecture of brain cortex in SCP-induced neurotoxic rats. GC-MS/MS identified dichloroacetic acid-tridec-2-ynyl ester, 6-hydroxymethylbicyclo [2.2.1]hept-2-ene-1-carboxylic acid-methyl ester, phytol acetate, n-hexadecanoic acid, β-sitosterol, quercetin-3-D-galactoside, stigmasterol, and genistin which were evaluated by *in silico* docking studies and found that, the drugs possess negative binding energies for AChE, BuChE, BACE1 and BACE2 indicating high affinity for the target enzymes in AD. From the proposed cellular mechanism of compounds in *G. repens* as shown in Fig. 5, further research is warranted to explore QSAR analysis of compounds, various signalling pathways, and mode of

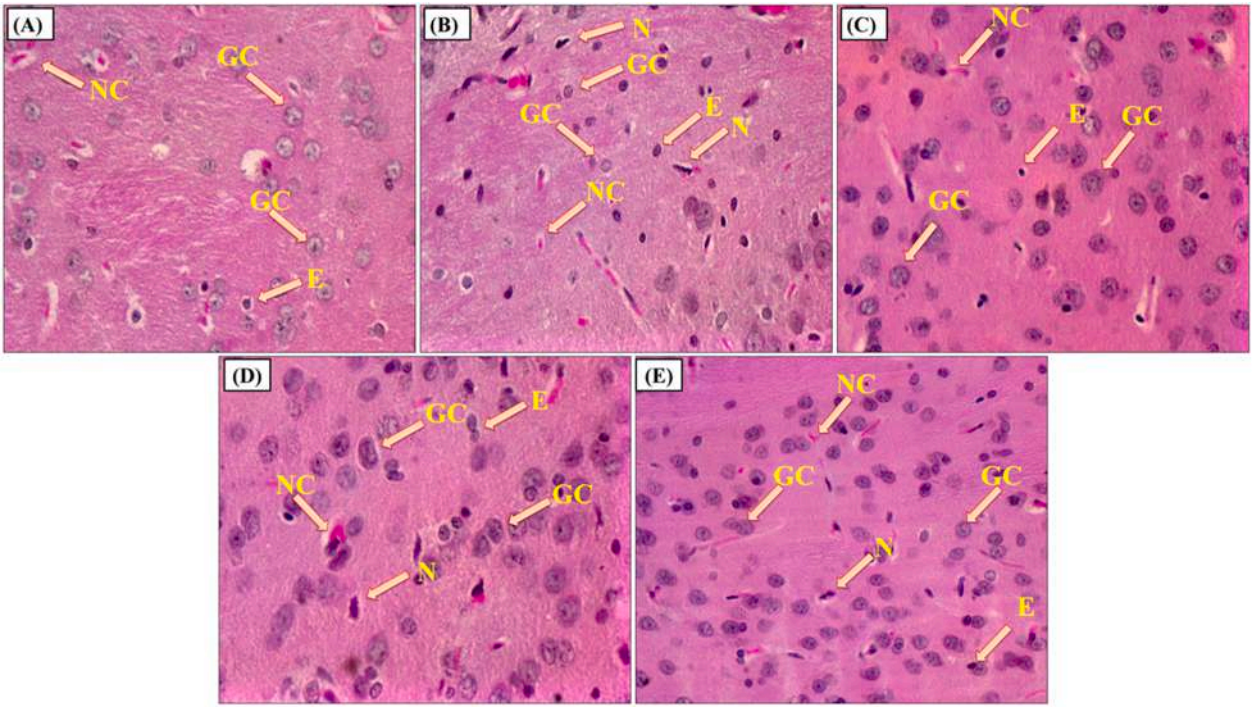

Fig. 4. Histopathological observations of brain cortex (T.S.) in scopolamine (SCP)-induced AD rats (40X, LYNX, Lawrence & Mayo, India). **A**. Brain tissue of normal control group showed normal histological findings with healthy cortical appearance with glial cells (GC), Neural cells (NC), Eosinophil (E) and no Necrotic cells (N). **B**. Toxicant control (SCP-induced) group revealed severe damage in normal cellular architecture as appearance of necrotic cells, shrunken glial cells and eosinophil along with the damaged neural cells and displayed marked neuronal degeneration (arrow) with neurophagia and gliosis. **C**. Positive control (Donepezil/DPZ treated) revealed the healing of eosinophils, glial, neural cells in comparison to SCP-induced group. **D**. GRHA-300 treated group showed moderate recovery of cellular architechture. **E**. GRHA-400 treated group recovered the cortex to normal status with appearance of healthy eosinophil, glial cells, neural cells with less necrotic cells against SCP-induced neurotoxic rats. GRHA, hydroalcohol fraction of *Geophila repens*.

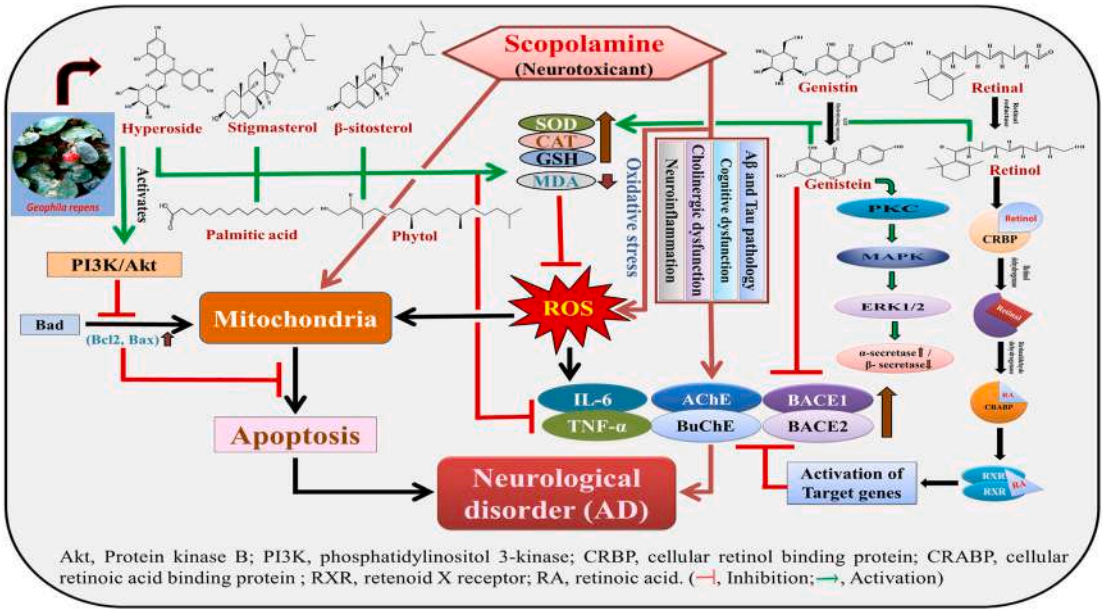

Fig. 5. Proposed schematic cellular reaction mechanism involved in SCP-induced neuropathological alternation. Reaction mechanism suggested the synergistic effect of prime molecules towards inhibition of ROS generation, mitochondrial dysfunction and markers in Alzheimer's disease (AChE, BuChE, BACE1 and BACE2).

action of lead compounds in cortex region of brain. This study highlights on design and development of novel multitargeted anti-Alzheimer's drugs in management of AD.

CRediT authorship contribution statement

Umesh Chandra Dash: Conceptualization, Writing – review & editing, Data curation, Writing – original draft, Study conception, review of literature, developing protocol, design and conduct experiment,

data interpretation, Manuscript preparation, reference set up. **Sandeep Kumar Swain:** Data curation, Writing – original draft, Conduct experiment, data interpretation, Manuscript preparation. **Satish Kanhar:** Data curation, Writing – original draft, Conduct experiment, data interpretation, Manuscript preparation. **Purusottam Banjare:** Data curation, Writing – original draft, Conduct experiment, data interpretation, Manuscript preparation. **Partha Pratim Roy:** Data curation, Writing – original draft, Conduct experiment, data interpretation, Manuscript preparation. **Jagneshwar Dandapat:** Data curation, Writing – original draft, Conduct experiment, data interpretation, Manuscript preparation. **Atish Kumar Sahoo:** Conceptualization, Writing – review & editing, Data curation, Writing – original draft, Study conception, review of literature, developing protocol, design and conduct experiment, data interpretation, Manuscript preparation, reference set up.

Declaration of competing interest

We wish to confirm that there are no known conflicts of interest associated with this publication and there has been no significant financial support for this work that could have influenced its outcome.

Acknowledgments

Funding provided by - Biju Patnaik Research Fellowship (BPRF) Scheme (grant no. 27562800382017/201152, ST Bhubaneswar, Dt. 23-02-2018), Science and Technology Department, Govt. of Odisha, Bhubaneswar, India.

References

Adebiyi, O.E., Olayemi, F.O., Olopade, J.O., Tan, N.H., 2019. Beta-sitosterol enhances motor coordination, attenuates memory loss and demyelination in a vanadium-induced model of experimental neurotoxicity. Pathophysiology 26, 21–29.

Al-Otaibi, S.N., Alshammari, G.M., AlMohanna, F.H., Al-Khalifa, A.S., Abdo Yahya, M., 2020. Antihyperlipidemic and hepatic antioxidant effects of Leek leaf methanol extract in high fat diet-fed rats. All. Life. 13, 373–385.

Aparna, V., Dileep, K.V., Mandal, P.K., Karthe, P., Sadasivan, C., Haridas, M., 2012. Anti-inflammatory property of n-hexadecanoic acid: structural evidence and kinetic assessment. Chem. Biol. Drug Des. 80, 434–439.

Babamiri, K., Nassab, R., 2010. Cosmeceuticals: the evidence behind the retinoids. Aesthetic Surg. J. 30, 74–77.

Barbier, P., Zejneli, O., Martinho, M., Lasorsa, A., Belle, V., Smet-Nocca, C., Tsvetkov, P. O., Devred, F., Landrieu, I., 2019. Role of Tau as a microtubule-associated protein: structural and functional aspects. Front. Aging Neurosci. 11, 1–14.

Basi, G., Frigon, N., Barbour, R., Doan, T., Gordon, G., McConlogue, L., Sinha, S., Zeller, M., 2003. Antagonistic effects of beta-site amyloid precursor protein-cleaving enzymes 1 and 2 on beta-amyloid peptide production in cells. J. Biol. Chem. 278, 31512–31520.

Belyaeva, O.V., Adams, M.K., Popov, K.M., Kedishvili, N.Y., 2019. Generation of retinaldehyde for retinoic acid biosynthesis. Biomolecules 10, 1–17.

Bhosale, U., Yegnanarayan, R., Prachi, P., Zambare, M., Somani, R.S., 2011. Study of CNS depressant and behavioral activity of an ethanol extract of *Achyranthes aspera* (Chirchita) in mouse model. Ann. Neurosci. 18, 44–47.

Birben, E., Sahiner, U.M., Sackesen, C., Erzurum, S., Kalayci, O., 2012. Oxidative stress and antioxidant defense. World. Allergy. Organ. J. 5, 9–19.

Bogie, J., Hoeks, C., Schepers, M., Tiane, A., Cuypers, A., Leijten, F., Chintapakorn, Y., Suttiyut, T., Pornpakakul, S., Struik, D., Kerksiek, A., Liu, H.B., Hellings, N., Martinez-Martinez, P., Jonker, J.W., Dewachter, I., Sijbrands, E., Walter, J., Hendriks, J., Groen, A., Staels, B., Lütjohann, D., Vanmierlo, T., Mulder, M., 2019. Dietary *Sargassum fusiforme* improves memory and reduces amyloid plaque load in an Alzheimer's disease mouse model. Sci. Rep. 9, 1–16.

Carta, G., Murru, E., Banni, S., Manca, C., 2017. Palmitic acid: physiological role, metabolism and nutritional implications. Front. Physiol. 8, 1–14.

Cole, S.L., Vassar, R., 2007. The Alzheimer's disease β-secretase enzyme. BACE1. Mol. Neurodegener. 2, 1–25.

Colovic, M.B., Krstic, D.Z., Lazarevic-Pasti, T.D., Bondžić, A.M., Vasic, V.M., 2013. Acetylcholinesterase inhibitors: pharmacology and toxicology. Curr. Neuropharmacol. 11, 315–335.

Dash, U.C., Kanhar, S., Dixit, A., Dandapat, J., Sahoo, A.K., 2019. Isolation, identification, and quantification of Pentylcurcumene from *Geophila repens*: a new class of cholinesterase inhibitor for Alzheimer's disease. Bioorg. Chem. 88, 1–11.

Dash, U.C., Sahoo, A.K., 2017. *In vitro* antioxidant assessment and a rapid HPTLC bioautographic method for the detection of anticholinesterase inhibitory activity of *Geophila repens*. J. Integr. Med. 15, 231–241.

DeTure, M.A., Dickson, D.W., 2019. The neuropathological diagnosis of Alzheimer's disease. Mol. Neurodegener. 14, 1–18.

Devi, K.P., Shanmuganathan, B., Manayi, A., Nabavi, S.F., Nabavi, S.M., 2017. Molecular and therapeutic targets of Genistein in Alzheimer's disease. Mol. Neurobiol. 54, 7028–7041.

Ellman, G.L., Courtney, K.D., Andres, V., Featherstone, R.M., 1961. A new and rapid colorimetric determination of acetylcholinesterase activity. Biochem. Pharmacol. 7, 88–95.

Ellman, G.L., 1959. Tissue sulfhydryl groups. Arch. Biochem. Biophys. 82, 70–77.

Francis, P.T., Palmer, A.M., Snape, M., Wilcock, G.K., 1999. The cholinergic hypothesis of Alzheimer's disease: a review of progress. J. Neurol. Neurosurg. Psychiatry 66, 137–147.

GBD 2016 Neurology Collaborators, 2019. Global, regional, and national burden of neurological disorders, 1990-2016: a systematic analysis for the global burden of disease study 2016. Lancet Neurol. 18, 459–480.

Giacobini, E., 2001. Selective inhibitors of butyrylcholinesterase: a valid alternative for therapy of Alzheimer's disease? Drugs Aging 18, 891–898.

Haider, S., Tabassum, S., Perveen, T., 2016. Scopolamine-induced greater alterations in neurochemical profile and increased oxidative stress demonstrated a better model of dementia: a comparative study. Brain Res. Bull. 127, 234–247.

Hesse, R., Wahler, A., Gummert, P., Kirschmer, S., Otto, M., Tumani, H., Lewerenz, J., Schnack, C., Arnim, C.A.F., 2016. Decreased IL-8 levels in CSF and serum of AD patients and negative correlation of MMSE and IL-1β. BMC Neurol. 16, 185.

Irizarry, M.C., Locascio, J.J., Hyman, B.T., 2001. Beta-site APP cleaving enzyme mRNA expression in APP transgenic mice: anatomical overlap with transgene expression and static levels with aging. Am. J. Pathol. 158, 173–177.

Islam, M.T., Ali, E.S., Uddin, S.J., Shaw, S., Islam, M.A., Ahmed, M.I., Chandra Shill, M., Karmakar, U.K., Yarla, N.S., Khan, I.N., Billah, M.M., Pieczynska, M.D., Zengin, G., Malainer, C., Nicoletti, F., Gulei, D., Berindan-Neagoe, I., Apostolov, A., Banach, M., Yeung, A.W.K., El-Demerdash, A., Xiao, J., Dey, P., Yele, S., Jóźwik, A., Strzałkowska, N., Marchewka, J., Rengasamy, K.R.R., Horbańczuk, J., Kamal, M.A., Mubarak, M.S., Mishra, S.K., Shilpi, J.A., Atanasov, A.G., 2018. Phytol: a review of biomedical activities. Food Chem. Toxicol. 121, 82–94.

Jamila, N., Yeong, K.K., Murugaiyah, V., Atlas, A., Khan, I., Khan, N., Khan, S.N., Khairuddean, M., Osman, H., 2015. Molecular docking studies and *in vitro* cholinesterase enzyme inhibitory activities of chemical constituents of *Garcinia hombroniana*. Nat. Prod. Res. 29, 86–90.

Jeong, S.H., 2018. Inhibitory effect of phytol on cellular senescence. Biomed. Dermatol. 2, 1–9.

Kanhar, S., Sahoo, A.K., Mahapatra, A.K., 2018. The ameliorative effect of *Homalium nepalense* on carbon tetrachloride-induced hepatocellular injury in rats. Biomed. Pharmacother. 103, 903–914.

Kim, S.J., Um, J.Y., Lee, J.Y., 2011. Anti-inflammatory activity of hyperoside through the suppression of nuclear factor-κB activation in mouse peritoneal macrophages. Am. J. Chin. Med. 39, 171–181.

Ku, S.K., Kwak, S., Kwon, O.J., Bae, J.S., 2014. Hyperoside inhibits high-glucose-induced vascular inflammation *in vitro* and *in vivo*. Inflammation 37, 1389–1400.

Lee, J.C., Park, J.H., Ahn, J.H., Park, J., Kim, I.H., Cho, J.H., Shin, B.N., Lee, T.K., Kim, H., Song, M., Cho, G.S., Kim, D.W., Kang, I.J., Kim, Y.M., Won, M.H., Choi, S.Y., 2018. Effects of chronic scopolamine treatment on cognitive impairment and neurofilament expression in the mouse hippocampus. Mol. Med. Rep. 17, 1625–1632.

Lin, H.W., Perez-Pinzon, M., 2013. The role of fatty acids in the regulation of cerebral vascular function and neuroprotection in ischemia. CNS Neurol. Disord. - Drug Targets 12, 316–324.

Maden, M., 2002. Retinoid signalling in the development of the central nervous system. Nat. Rev. Neurosci. 3, 843–853.

Rajashri, K., Mudhol, S., Peddha, M.S., Borse, B.B., 2020. Neuroprotective effect of spice oleoresins on memory and cognitive impairment associated with scopolamine-induced Alzheimer's disease in rats. ACS Omega 5, 30898–30905.

Sahoo, A.K., Dandapat, J., Dash, U.C., Kanhar, S., 2018. Features and outcomes of drugs for combination therapy as multi-targets strategy to combat Alzheimer's disease. J. Ethnopharmacol. 215, 42–73.

Santos, C.C., Salvadori, M.S., Mota, V.G., Costa, L.M., De-Almeida, A.A., De-Oliveira, G. A., Costa, J.P., De-Sousa, D.P., De-Freitas, R.M., De-Almeida, R.N., 2013. Antinociceptive and antioxidant activities of phytol *in vivo* and *in vitro* models. Neuroscience J. 2013, 1–9.

Sethuraman, S., Boovaragamoorthy, G.M., Kaliannan, T., Sethuraman, V., Kandasamy, R., Kasi, P.D., 2020. Phytol loaded PLGA nanoparticles ameliorate scopolamine-induced cognitive dysfunction by attenuating cholinesterase activity, oxidative stress and apoptosis in Wistar rat. Nutr. Neurosci. 14, 1–17.

Sivarajan, V.V., Balachandran, I., 1994. Ayurvedic Drugs and Their Plant Sources. Oxford and IBH Publishing, New Delhi, p. 201.

Subramoniam, A., Rajasekharan, S., Vinod, K.T.G., Pushpangadan, P., 1998. Hepatoprotective activity of *Geophila reniformis* (Tender leaves) against paracetamol or carbon tetrachloride-induced hepatic damage in rats. In: Murali TS. Holistic Life and Medicine. Arya Vaidya Sala, Kottakkal, pp. 187–193.

Sun, J., Li, X., Liu, J., Pan, X., Zhao, Q., 2019. Stigmasterol exerts neuro-protective effect against ischemic/reperfusion injury through reduction of oxidative stress and inactivation of autophagy. Neuropsychiatric Dis. Treat. 15, 2991–3001.

Swain, S.K., Dash, U.C., Kanhar, S., Sahoo, A.K., 2020. Ameliorative effects of *Hydrolea zeylanica* in streptozotocin-induced oxidative stress and metabolic changes in diabetic rats. J. Ethnopharmacol. 247, 112257.

Uddin, M.S., Kabir, M.T., 2019. Emerging signal regulating potential of Genistein against Alzheimer's disease: a promising molecule of interest. Front. Cell. Dev. Biol. 7, 1–12.

Upadhyay, P., Shukla, R., Tiwari, K.N., Dubey, G.P., Mishra, S.K., 2020. Neuroprotective effect of *Reinwardtia indica* against scopolamine induced memory-impairment in rat by attenuating oxidative stress. Metab. Brain Dis. 35, 709–725.

Wang, W.Y., Tan, M.S., Yu, J.T., Tan, L., 2015. Role of pro-inflammatory cytokines released from microglia in Alzheimer's disease. Ann. Transl. Med. 3, 1–15.
Woo, Y., Lim, J.S., Oh, J., Lee, J.S., Kim, J., 2020. Neuroprotective effects of *Euonymus alatus* extract on scopolamine-induced memory deficits in mice. Antioxidants 9, 1–14.
Wright, J.R., Colby, H.D., Miles, P.R., 1981. Cytosolic factors which affect microsomal lipid peroxidation in lung and liver. Arch. Biochem. Biophys. 206, 296–304.
Yadang, F.S.A., Nguezeye, Y., Kom, C.W., Betote, P.H.D., Mamat, A., Tchokouaha, L.R.Y., Taiwé, G.S., Agbor, G.A., Bum, E.N., 2020. Scopolamine-induced memory impairment in mice: neuroprotective effects of *carissa edulis* (Forssk.) Valh (Apocynaceae) aqueous extract. Int. J. Alzheimer's Dis. 2020, 1–10.
Zeng, K.W., Wang, X.M., Ko, H., Kwon, H.C., Cha, J.W., Yang, H.O., 2011. Hyperoside protects primary rat cortical neurons from neurotoxicity induced by amyloid β-protein via the PI3K/Akt/Bad/Bcl (XL)-regulated mitochondrial apoptotic pathway. Eur. J. Pharmacol. 672, 45–55.
Zhang, Y., Wang, Q., Chen, H., Liu, X., Lv, K., Wang, T., Wang, Y., Ji, G., Cao, H., Kan, G., Li, Y., Qu, L., 2018. Involvement of cholinergic dysfunction and oxidative damage in the effects of simulated weightlessness on learning and memory in rats. BioMed Res. Int. 2018, 1–11.
Zipp, F., Aktas, O., 2006. The brain as a target of inflammation: common pathways link inflammatory and neurodegenerative diseases. Trends Neurosci. 29 (9), 518–527.
Zhou, L., Tan, S., Shan, Y.L., Wang, Y.G., Cai, W., Huang, X.H., Liao, X.Y., Li, H.Y., Zhang, L., Zhang, B.J., Lu, Z.Q., 2016. Baicalein improves behavioral dysfunction induced by Alzheimer's disease in rats. Neuropsychiatric Dis. Treat. 12, 3145–3152.